Fachtagung "Experimentelle Strömungsmechanik"
7.–9. September 2021, Bremen

Messung der Geschwindigkeits- und Partikeldichteverteilung in Partikelbeladene Rohrströmungen mittels MRV

MRV Measurement of Velocity and Particle Distribution within Particle-Laden Pipe Flows

D. Frank[1], W. Hogendoorn[2], M. Bruschewski[1], S. Grundmann[1], C. Poelma[2]
[1]Universität Rostock, Lehrstuhl Strömungsmechanik, Albert-Einstein-Str. 2, 18059 Rostock
[2]Delft University of Technology, Faculty Mechanical, Maritime and Materials Engineering, Leeghwaterstraat 39, 2628 CA Delft – The Netherlands

Magnetic resonanz velocimetry, particle-laden flows, transition to turbulence
Magnet-Resonanz-Velocimetrie, Partikelbeladene Strömung, Transition

Zusammenfassung

Das Strömungsverhalten von partikelbeladenen Strömungen ist für verschiedene biologische, chemische und industrielle Anwendungen von Interesse. Sowohl das Transitionsverhalten dieser Strömungen als auch die Partikelmigration innerhalb der Suspensionen bleiben bis zu diesem Zeitpunkt relevant. Trotz erheblicher Forschungsanstrengungen sind viele Aspekte dieser Phänomene noch unbekannt oder zumindest aufklärungsbedürftig. Um unser Verständnis des Partikelmigrationsverhaltens innerhalb solcher Strömungen zu vertiefen, sind dreidimensionale nichtinvasive Messungen erforderlich. Aufgrund der Opazität dichter Suspensionen sind optische Messungen sehr anspruchsvoll, was eine Gelegenheit für alternative Messmethoden bietet die Datenlücke zu füllen.
Mittels Magnetresonanz-Velocimetrie (MRV) sind wir in der Lage, hochauflösende zeitgemittelte 2D1C Geschwindigkeits- und Partikelverteilungsdaten einer partikelbeladenen Rohrströmung darzustellen. Die Suspension besteht aus auftriebsneutralen, kugelförmigen Polystyrolpartikeln ($D/d = 17.3$), die in einer Newtonschen Flüssigkeit suspendiert sind. Es wurden Partikelvolumenanteile von bis zu 50% sowohl in laminaren als auch in turbulenten Strömungsbereichen erreicht.
Die Daten geben Aufschluss über das Migrationsverhalten der Partikel und deren Einfluss auf die Geschwindigkeitsverteilung. Sowohl eine ringförmige Struktur als auch eine starke Partikelmigration in Richtung Rohrmitte sind zu beobachten. Sobald die Suspension eine dichte Partikelpackung (68%) in der Mitte des Rohres erreicht, kann außerdem das Auftreten mehrerer ringförmiger Strukturen festgestellt werden. Die Verbindung dieser drei Merkmale mit der Reynoldszahl kann zu unserem theoretischen Verständnis dieser Strömungen beitragen. Darüber hinaus bietet die hohe Qualität und das breite Datenspektrum gute Validierungsfälle für numerische und empirische Modelle.

Abstract

Particle-laden flow behaviour is of interest for various biological, chemical, and industrial applications. Both the transitional behaviour of these flows and the particle migration within the suspensions remain relevant until this date. Despite considerable research efforts, many aspects of these phenomena remain unknown or at least require clarification. In order to further our understanding of the particle behaviour within such flows, three-dimensional non-invasive

measurements are required. Due to the opacity of dense suspensions, optical measurements become more challenging, which opens the door for alternative techniques.
Using magnetic resonance velocimetry (MRV), we are able to present high-resolution time-averaged 2D1C velocity and particle distribution data of a particle-laden pipe flow. The suspension consists of neutrally buoyant, spherical polystyrene particles ($D/d = 17.3$) suspended in a Newtonian fluid. Average particle volume fractions of up to 50% across both laminar and turbulent flow regimes were reached.
The data provides insight into the migratory behaviour of the particles and their influence on the velocity distribution. Both, a ring-like structure close to the wall and a strong migratory pull towards the centre can be observed. Additionally, once the suspension reaches high particle packing (68%) in the centre of the pipe, the appearance of multiple ring-like structures can be detected. The connection of these three characteristics to the Reynolds number can contribute to our theoretical understanding of these flows. Furthermore, the high quality and wide range of data provide good validation cases for numerical and empirical models.

Introduction

Particle-laden flows can be defined by several characteristics. One important characteristic is the preferential migratory behaviour of the particles. One particular example of this is the tubular pinch effect in dilute suspensions (Segré and Silberberg, 1961). This is the result of the Saffman lift, which pulls the particles into an equilibrium somewhere between the centre axis of the pipe and the pipe wall. However, when dealing with higher particle concentrations, we have to consider particle interactions as a dominant factor within the particle migration effects. Several experimental studies have shown a competition between the forces pulling the particles towards the wall and the forces pulling the particles towards the centre (Matas et al. 2004, Costa et al. 2018). Due to the challenging nature to determine the particle distribution within dense suspensions, other methods such as MRV became of interest (Hampton et al. 1997; Han et al. 1999).
This article presents MRV derived measurement data of suspensions with average volume fractions of up to $\phi = 0.5$ within laminar, transitional, and turbulent flow regimes.

Materials and Methods

The suspension consists of spherical polystyrene particles in a density-matched Newtonian fluid. The average particle diameter is $d = 1.75 \pm 0.12\, mm$. The density of the fluid was matched with the particle density by adding glycerine, until a mixture with 18% glycerine concentration in mass was reached. Furthermore, $1\, g/L$ Copper(II) sulfate was added as contrast agent.
The flow domain consists of an acrylic tube with a measured inner diameter of $D = 30.35 \pm 0.12\, mm$. The measurement setup is shown in figure 1 and consists of a Mono Compact-Range progressive cavity pump (AxFlow, Düsseldorf, Germany), with a frequency controller as well as a bypass, and throttle to achieve the desired flow conditions. A converging inlet chamber is used to ensure smooth inlet conditions. After this inlet chamber, a trip ring is placed to trigger the transition of turbulence at a single-phase Reynolds number of around 2000. The distance between the trip ring and the isocentre of the scanner is $132D$. The temperature was measured at the pump inlet and a FT402 cooling unit (Julabo, Seelbach, Germany) was placed in the reservoir to minimise the temperature increase over longer measurement cycles. These temperature measurements were used to adjust the viscosity of water accordingly. Additionally, the viscosity of the suspension is corrected using the Eilers's Model (Eilers 1941),

$$\frac{\mu}{\mu_0} = \left(1 + 1.125 \frac{\phi}{1 - \frac{\phi}{0.64}}\right)^2 \qquad (1)$$

with μ_0 being the temperature-adjusted single-phase viscosity and ϕ the average particle volume fraction. The viscosity of particle-laden flows rises for increasing particle volume fractions, which in turn means an increased flow rate required to reach equal Reynolds numbers. The pump reached a limit at a volume fraction $\phi = 0.5$ and Reynolds number $Re = 560$.

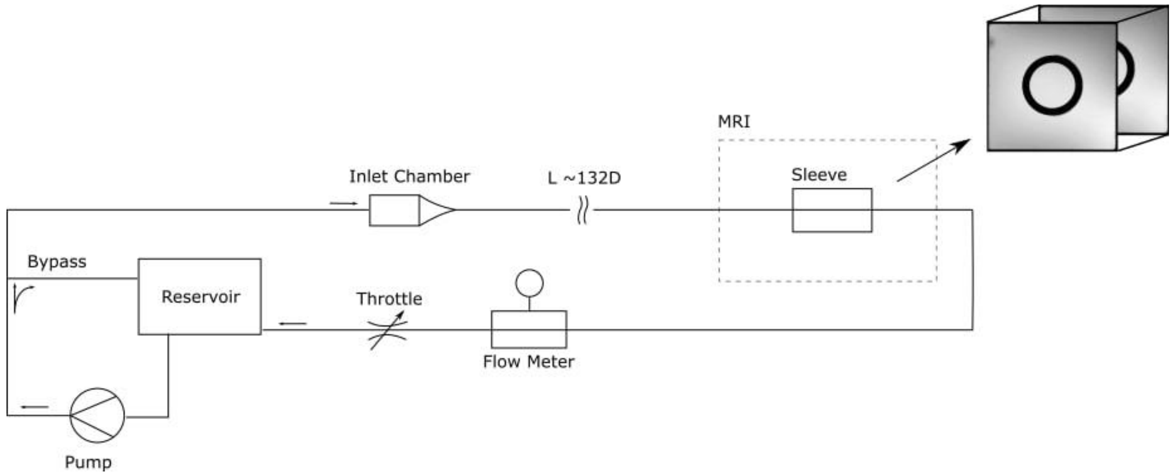

Fig. 1: Measurement setup used for the MRV measurements.

The data is obtained using a Siemens 3T Magnetom Tim Trio (Siemens, Erlangen, Germany). The scanner has a maximum gradient amplitude of 40 mTm^{-1} and a maximum gradient slew rate of 200$Tm^{-1}s^{-1}$. The general parameters are listed in table 1. Note, that a non-isotropic resolution was chosen, which behaves similar to a spatial average along the axial direction.

Tab. 1: Parameters of the MRV measurement

Parameter	**Value**
Matrix size	640 x 640 x 1
Non-isotropic resolution	0.3 x 0.3 x 50 mm
Repetition time	22 ms
RF flip angle	5°
Receiver bandwidth	280 Hz Pixel^{-1}
VENC	0.1 - 0.8 m/s
Number of averages	32
Total acquisition time	30 min

The local particle volume fraction, φ, can be calculated using a reference measurement containing the single-phase fluid only. This assumes that the signal loss between the two measurements is proportional to the number of particles in the fluid. However, since these were measured several hours apart, we have to take a possible temporal magnetic shift into account. For this reason, a reference single-phase fluid was placed in a 'sleeve' around the pipe to provide a reference for all measurements. The final formula for φ is,

$$\varphi(x, y) = 1 - \frac{M(x,y)/\overline{M_{sleeve}}}{M(x,y)_{ref}/\overline{M_{sleeve,ref}}} \tag{2}$$

where M represents the image magnitude, while $\overline{M_{sleeve}}$ is the average magnitude of the sleeve.

Results

The results presented in this section can be split into two categories: velocity data and particle concentration data. The time-averaged velocity data shows the influence of the particles on the overall velocity distribution. However, due to MRV only receiving a signal of the liquid phase within the suspension, it cannot determine the particle velocity. The time-averaged particle distribution shows the migratory preferences of the particles within the different flow regimes. All the data presented in the profile plots were radially averaged and interpolated onto a radial grid.

MRV velocity data

In order to provide a reference, a particle-free flow ($\phi = 0$) and a low concentration particle-laden flow ($\phi = 0.1$) are compared across laminar, transitional, and turbulent regimes and presented in figure 2. The comparison shows that the single-phase flow and the particle-laden flow are virtually identical across both laminar and turbulent regimes. Note, that the particle-laden case within the transitional regime seems to transition earlier than the single-phase flow (see figure 2: $\phi = 0.1 \mid Re = 2000$ versus $\phi = 0 \mid Re = 2000$). This is in good agreement with literature (Matas et al. 2003; Hof et al. 2006; Hogendoorn und Poelma 2018; Hogendoorn et al. 2021), which show that the particle-induced perturbations cause a decrease of the critical Reynolds number.

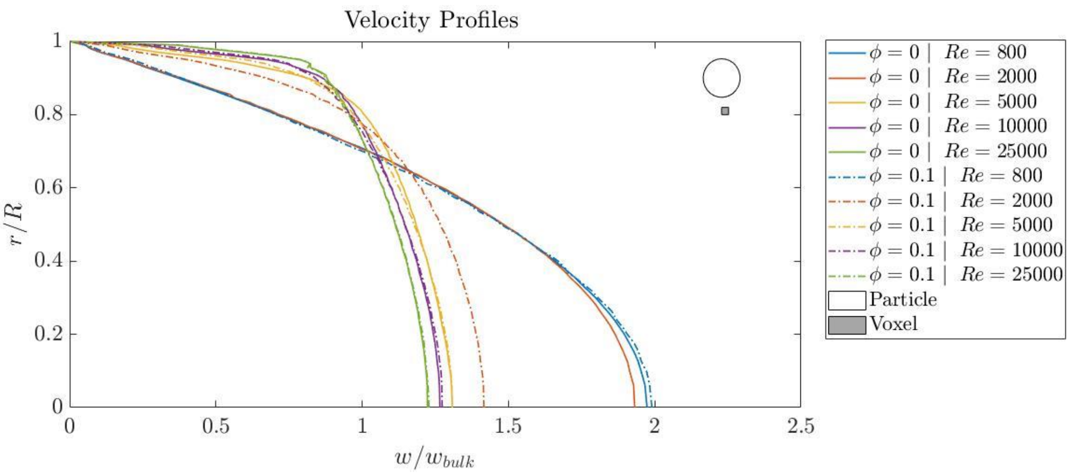

Fig. 2: Comparison of the velocity profiles between a single-phase flow and a particle-laden flow with a particle volume fraction $\phi = 0.1$. The y-axis represents the normalized radius, while the x-axis describes the axial velocity w normalized by the bulk velocity w_{bulk}.

A similar comparison for the higher volume fractions is shown in figure 3. A few observations can be made from this data. First, for increasing ϕ, an overall flattening of the velocity profile can be seen, even for low Reynolds numbers. Interestingly, for higher Reynolds numbers ($Re = 2000$ & $Re = 5000$), the maximum velocity (i.e. at the centreline) of the $\phi = 0.2$ and $\phi = 0.3$ cases exceed the $\phi = 0.1$ case. This can be explained by the particle distribution data, presented in the following section.

GALA e.V., Karlsruhe, Germany, ISBN 978-3-9816764-7-1

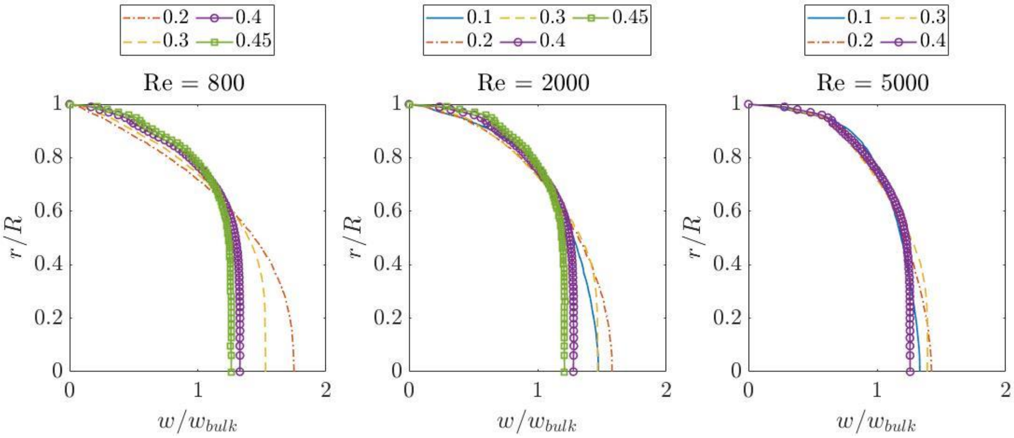

Fig. 3: Velocity profiles from the liquid phase within particle-laden pipe flows. The y-axis represents the normalized radius, while the x-axis describes the axial velocity w normalized by the bulk velocity w_{bulk}. The numbers in the legend represent the average volume fraction ϕ.

MRV particle distribution

The particle distribution of all measurements is shown in fig. 4. Here, we can see that for low volume fractions ($\phi = 0.1$) the particles have a relatively homogenous distribution. At higher concentrations, the migration towards the centre becomes more dominant. The data confirms previous observations, which suggest that high inertia flows reinforce the migration towards the wall, while higher volume fractions reinforce the migration towards the centre (Costa et al. 2018; Matas et al. 2004). Interestingly, the cases were the maximum velocity in the centre is increased ($\phi = 0.2$ & $\phi = 0.3$), also have a particle concentration peak in the centre axis.

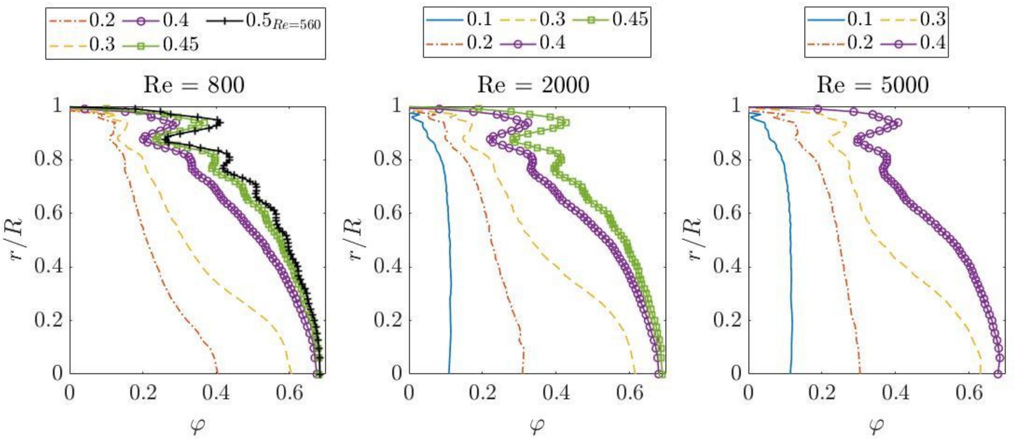

Fig. 4: Illustration showing the time-averaged local particle volume fraction φ distribution for three different Reynolds numbers. The numbers in the legend represent the average volume fraction ϕ. The $\phi = 0.5$ case is included in the $Re = 800$ plot, but it should be mentioned that the Reynolds number in that case is slightly lower ($Re = 560$).

The increase of the average particle concentration is linked to an increase in the number of ring-like structures. These seem to become more prominent, once a maximum concentration of $\varphi \approx 0.68$ is reached in the centre of the pipe. These structures are shown in more detail in fig. 4. They are most likely caused by the movement limitation in radial direction, essentially trapping the particles between the centre and the wall. Finally, we can see that buoyancy plays a significant role up to $\varphi = 0.2$, but diminishes for higher concentrations where particle interactions become more dominant.

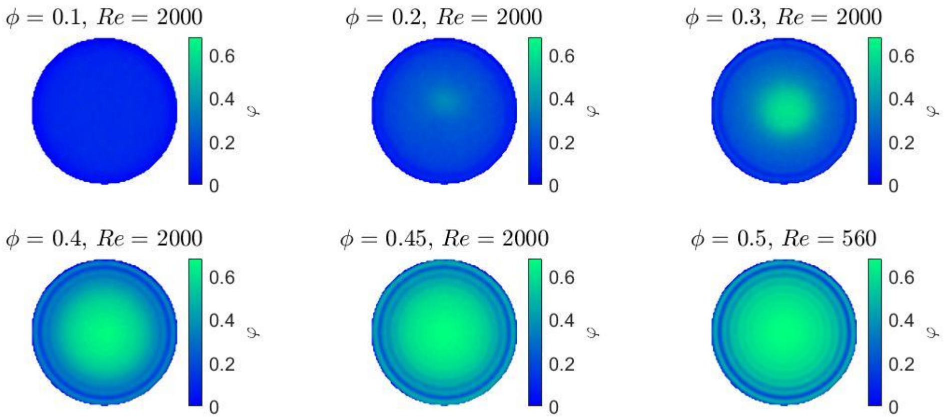

Fig. 4: Contour plots of the time-averaged local particle volume fraction, determined using eq. 2. Green marks dense particle concentrations while blue indicates low particle concentrations. The illustration shows the particle migration effects for the Reynolds number $Re = 2000$ for various particle volume fractions. $\phi = 0.5$ is the exception since $Re > 560$ could not be reached by the measurement setup. The contours show that at higher concentrations ($\phi \geq 0.4$), multiple ring-like structures are formed.

Discussion

The data for the lower volume fractions $\phi < 0.4$ confirms the general trends observed by others (Han et al. 1999; Hampton et al. 1997; Lyon und Leal 1998). Additionally, the data for higher concentration suspensions shows that a behaviour change appears to happen once the particle concentration within the pipe centre reaches a maximum of 68%. Experiments have shown that the densest random closed packing of monodisperse spheres typically occurs close to $\phi_c \approx 0.64$ (Bernal und Mason 1960; Scott und Kilgour 1969). However, polydispersity can have a significant impact on the packing density, which makes a maximum packing of $\phi_c \approx 0.68$ feasible (Desmond und Weeks 2014). Once this number is reached, the particles are limited in their radial movement and forced into circular equilibria. The effects of the maximum particle packing within a particle-laden flow might play an important role for dense particle laden flows and will require more research to be fully understood.

Furthermore, the effects of the particles on the velocity distribution require more clarification and thus invite further research. Currently, additional measurements on this topic are being pursued.

Conclusion

The competing nature of the migration forces towards the wall and towards the centre of the pipe has been demonstrated in high-resolution MRV images. Due to the non-isotropic resolution, which essentially behaves like a spatial average along the axial direction, it was possible to achieve high signal-to-noise ratios while maintaining a high in-plane resolution. This data is therefore well suited as validation data for numerical simulations und to further insight in the underlying physics.

The time-averaged 2D1C velocity data provides insight into the complex flow behaviour of the single-phase fluid within the particle-laden flows. The particle concentration data confirms general trends observed in literature. Furthermore, the appearance of multiple ring-like structures within dense suspensions has been documented. This phenomenon invites further research on its connection to flow behaviour and turbulence transition of high density particle-laden flows.

Literature

Bernal, J. D., Mason, J., 1960: "Packing of spheres: co-ordination of randomly packed spheres", In: *Nature* 188 (4754), S. 910–911. DOI: 10.1038/188910a0
Costa, P., Picano, F., Brandt, L., Breugem, W.-P., 2018: " Effects of the finite particle size in turbulent wall-bounded flows of dense suspensions", In: *J. Fluid Mech.* 843, S. 450–478. DOI: 10.1017/jfm.2018.117.
Desmond, K. W., Weeks, E. R., 2014: "Influence of particle size distribution on random close packing of spheres", In: *Physical review. E, Statistical, nonlinear, and soft matter physics* 90 (2), S. 22204. DOI: 10.1103/PhysRevE.90.022204.
Eilers, H., 1941: "Die Viskosität von Emulsionen hochviskoser Stoffe als Funktion der Konzentration", In: *Kolloid-Zeitschrift* 97 (3), S. 313–321. DOI: 10.1007/BF01503023.
Hampton, R. E., Mammoli, A. A., Graham, A. L., Tetlow, N., Altobelli, S. A., 1997: "Migration of particles undergoing pressure-driven flow in a circular conduit", In: *Journal of Rheology* 41 (3), S. 621–640. DOI: 10.1122/1.550863.
Han, M., Kim, C., Kim, M, Lee, S., 1999: "Particle migration in tube flow of suspensions", In: *Journal of Rheology* 43 (5), S. 1157–1174. DOI: 10.1122/1.551019.
Hof, B., Westerweel, J., Schneider, T. M., Eckhardt, B., 2006: " Finite lifetime of turbulence in shear flows", In: *Nature* 433 (7107), S. 59–62. DOI: 10.1038/nature05089.
Hogendoorn, W., Chandra, B., Poelma, C., 2021: "Universal scaling for the onset of turbulence in particle-laden flows", Available online: https://arxiv.org/pdf/2104.14883.
Hogendoorn, W., Poelma, C., 2018: "Particle-laden pipe flows at high volume fractions show transition without puffs", In: *Physical review letters* 121 (19), 1-5. DOI: 10.1103/PhysRevLett.121.194501.
Lyon, M. K., Leal, L. G., 1998: "An experimental study of the motion of concentrated suspensions in two-dimensional channel flow", Part 1. Monodisperse systems. In: *J. Fluid Mech.* 363, S. 25–56. DOI: 10.1017/S0022112098008817.
Matas, J.-P., Morris, J. F., Guazzelli, E., 2003: "Transition to turbulence in particulate pipe flow", In: *Physical review letters* 90 (1), S. 14501. DOI: 10.1103/PhysRevLett.90.014501.
Matas, J.-P., Morris, J. F., Guazzelli, E., 2004: "Lateral forces on a sphere", In: *Oil & Gas Science and Technology - Rev. IFP* 59 (1), S. 59–70. DOI: 10.2516/ogst:2004006.
Scott, G. D., Kilgour, D. M., 1969: "The density of random close packing of spheres", In: *J. Phys. D: Appl. Phys.* 2 (6), S. 863–866. DOI: 10.1088/0022-3727/2/6/311.
Segré, G., Silberberg, A., 1961: "Radial particle displacements in Poiseuille flow of suspensions", In: *Nature* 189 (4760), S. 209–210. DOI: 10.1038/189209a0.